




Zinc finger protein E4F1 cooperates with PARP-1 and BRG1 to promote DNA double-strand break repair

Céline Moison^a, Jalila Chagraoui^a, Marie-Christine Caron^{b,c}, Jean-Philippe Gagné^{c,d} , Yan Coulombe^{b,c}, Guy G. Poirier^{c,d}, Jean-Yves Masson^{b,c}, and Guy Sauvageau^{a,e,f,1}

^aMolecular Genetics of Stem Cells Laboratory, Institute for Research in Immunology and Cancer, University of Montreal, Montreal, QC H3T 1J4, Canada; ^bGenome Stability Laboratory, Oncology Division, CHU de Québec Research Center, Québec City, QC G1R 3S3, Canada; ^cDepartment of Molecular Biology, Medical Biochemistry and Pathology, Laval University Cancer Research Center, Québec City, QC G1V 0A6, Canada; ^dOncology Division, CHU de Québec Research Center, Québec City, QC G1V 4G2, Canada; ^eDepartment of Medicine, Faculty of Medicine, University of Montreal, Montreal, QC H3T 1J4, Canada; and ^fDivision of Hematology, Maisonneuve-Rosemont Hospital, Montreal, QC H1T 2M4, Canada

Edited by Stephen C. West, The Francis Crick Institute, London, United Kingdom, and approved February 8, 2021 (received for review September 14, 2020)

Zinc finger (ZnF) proteins represent one of the largest families of human proteins, although most remain uncharacterized. Given that numerous ZnF proteins are able to interact with DNA and poly(ADP ribose), there is growing interest in understanding their mechanism of action in the maintenance of genome integrity. We now report that the ZnF protein E4F transcription factor 1 (E4F1) is an actor in DNA repair. Indeed, E4F1 is rapidly recruited, in a poly(ADP ribose) polymerase (PARP)-dependent manner, to DNA breaks and promotes ATR/CHK1 signaling, DNA-end resection, and subsequent homologous recombination. Moreover, we identify E4F1 as a regulator of the ATP-dependent chromatin remodeling SWI/SNF complex in DNA repair. E4F1 binds to the catalytic subunit BRG1/SMARCA4 and together with PARP-1 mediates its recruitment to DNA lesions. We also report that a proportion of human breast cancers show amplification and overexpression of *E4F1* or *BRG1* that are mutually exclusive with *BRCA1/2* alterations. Together, these results reveal a function of E4F1 in the DNA damage response that orchestrates proper signaling and repair of double-strand breaks and document a molecular mechanism for its essential role in maintaining genome integrity and cell survival.

E4F1 | double-strand break | PARP-1 | BRG1 | breast cancer

Cycling cells acquire numerous DNA lesions under physiological conditions and thus require functional DNA damage response (DDR) pathways to support proper DNA repair. Hundreds of proteins orchestrate the DDR in time and space. The repair process ranges from very early events such as the sensing of DNA lesions by DNA-dependent poly(ADP ribose) polymerases (PARPs) to late steps in chromatin restoration. In between, the interactions of a plethora of proteins lead to the coordination of signaling through multiple pathways that facilitate chromatin remodeling and decondensation to promote access of key factors to DNA lesions and the recruitment of DNA repair proteins.

E4F transcription factor 1 (E4F1) is a ubiquitously expressed transcriptional regulator that plays a critical role in cell cycle control and proliferation. In normal cell physiology, *E4F1* is essential for both embryonic development and adult tissue homeostasis. Notably, p53 and pRB count among E4F1 direct interacting partners to fulfill its cell cycle regulatory functions (1–3). Phenotypically, *E4F1*-deficient cells exhibit mitotic defects, chromosomal missegregation, and increased apoptosis (4, 5). Our group also has reported accumulation in S phase, reduction in replication fork rate, and decreased BrdU incorporation in *E4F1*-null mouse embryonic fibroblasts (MEFs), all indicative of ongoing replicative stress (5).

Emerging roles of noncanonical repair proteins, such as transcriptional regulators or zinc fingers (ZnFs), in DNA repair are particularly intriguing. For example, the multifunctional E2F1 protein, beyond its well-known role in transcription, also promotes DNA repair with its pRB partner (6, 7). A growing body of literature also describes the role of ZnF proteins in maintaining genome integrity (8), including proteins acting as

activators or repressors of homologous recombination (HR) repair. For example, ZPET/ZNF280C was recently described as a repressor of HR through its binding to single-stranded DNA (ssDNA) (9), ZNF830 facilitates HR by regulating CtIP recruitment to DNA lesions (10), and ZMYM3 regulates BRCA1 recruitment to double-strand breaks (DSBs) (11).

Taking into consideration the impact of E4F1 on genome integrity and its interaction with CHK1 and p53, we hypothesized that E4F1 may play a direct role in DDR. The results presented herein indeed define E4F1 as a player in DSB repair that promotes γ H2AX clearance, transcriptional silencing, DNA-end resection and HR. These findings provide a molecular explanation for the essential role of E4F1 in DDR-associated cell cycle arrest and survival.

Results

Human E4F1-Deficient Cells Display Impaired Survival, Replicative Stress, and Defects in DNA Repair. To investigate *E4F1* cellular functions, we first used the human osteosarcoma U2OS cell line in which *E4F1* expression is abolished by doxycycline-inducible CRISPR-Cas9 (Fig. 1A). In line with its essential role in proliferating cells, loss of *E4F1* produced a marked impairment in cell proliferation and cell cycle mostly characterized by G2 accumulation, reduced EdU incorporation, and delayed S phase progression (Fig. 1B and C and *SI Appendix, Fig. S1A*). Increased phosphorylation of p53 at serine 15 was also indicative of important

Significance

Cycling cells acquire numerous DNA lesions under physiological conditions and thus require functional DNA damage response (DDR) pathways to support proper DNA repair. Hundreds of proteins orchestrate the DDR in time and space from very early events, such as the sensing of DNA lesions by DNA-dependent poly(ADP-ribose) polymerases (PARPs) to late steps in chromatin restoration. Here we define a function of E4F1 in double-strand break repair. We show that E4F1 is rapidly recruited to DNA lesions by PARP-1, where it promotes γ H2AX clearance, transcriptional silencing, DNA-end resection, and homologous recombination. These data provide an unsuspected molecular explanation for the essential role of E4F1 in DDR-associated cell cycle arrest and survival.

Author contributions: C.M., J.C., J.-P.G., G.G.P., J.-Y.M., and G.S. designed research; C.M., M.-C.C., J.-P.G., and Y.C. performed research; C.M., M.-C.C., J.-P.G., and Y.C. analyzed data; and C.M., J.C., J.-P.G., and G.S. wrote the paper.

The authors declare no competing interest.

This article is a PNAS Direct Submission.

Published under the PNAS license.

¹To whom correspondence may be addressed. Email: guy.sauvageau@umontreal.ca.

This article contains supporting information online at <https://www.pnas.org/lookup/suppl/doi:10.1073/pnas.2019408118/-DCSupplemental>.

Published March 10, 2021.

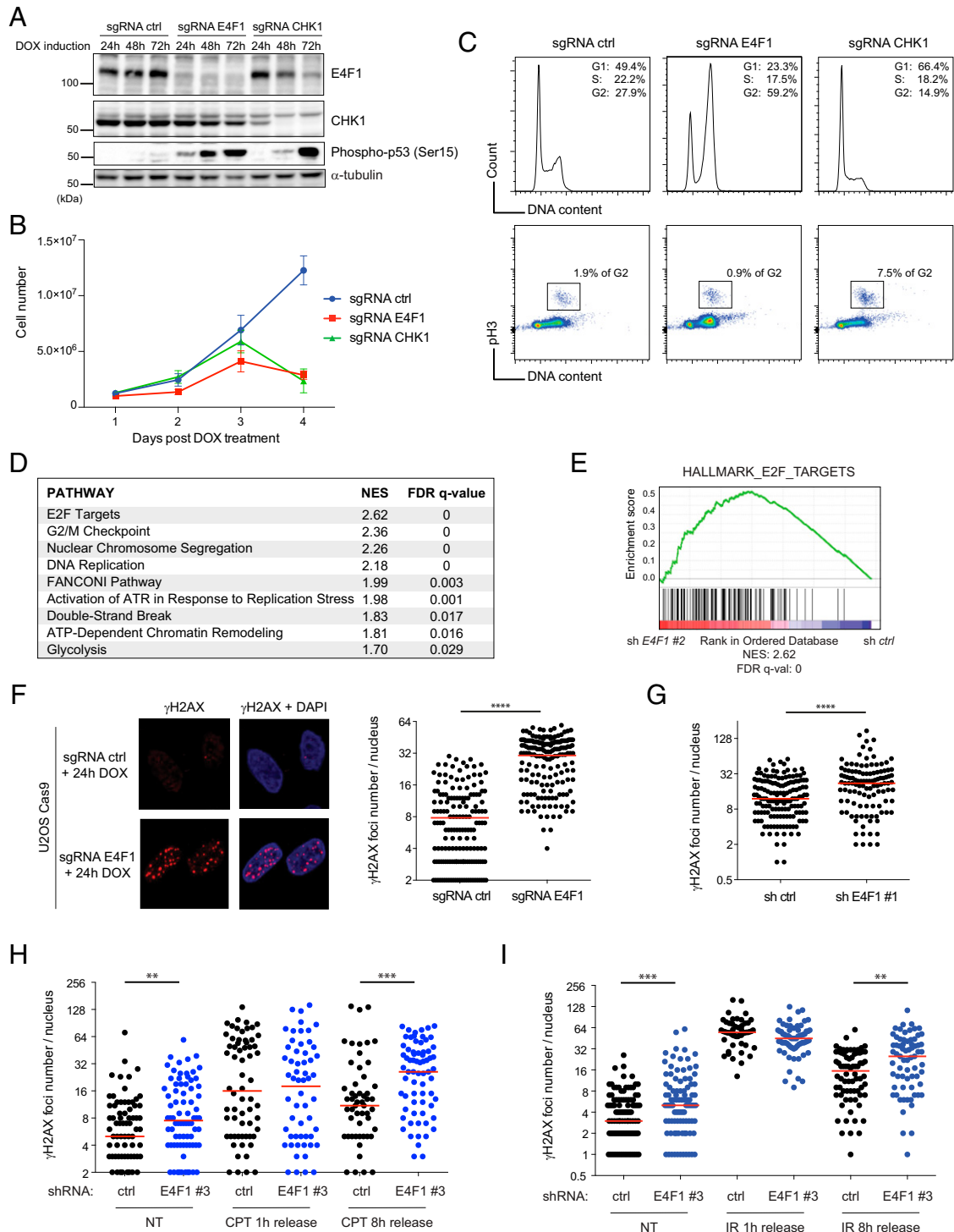


Fig. 1. Human E4F1-deficient cells display impaired survival, replicative stress, and defects in DNA repair. (A) Immunoblot of total E4F1, CHK1, and phospho-p53 (ser15) proteins in U2OS cells after doxycycline-induced Cas9 expression. Cells constitutively expressed the indicated sgRNA. α -tubulin served as a loading control. (B) U2OS cells expressing the indicated sgRNA were monitored for cell proliferation after doxycycline-mediated Cas9 expression. Cells were seeded in 12-well plates and counted at the indicated time. $n = 3$. Error bars represent mean \pm SD. (C) At 72 h after Cas9 induction, U2OS cells expressing the indicated sgRNAs were fixed and analyzed by flow cytometry for cell cycle distribution and phospho-(ser10) H3 positivity (mitosis vs. G2). (D) List of transcriptomic signatures associated with E4F1 loss in U2OS cells and determined by GSEA. (E) GSEA plot comparing U2OS cells expressing control or E4F1 shRNAs. NES, normalized enrichment score; FDR, false discovery rate. (F) At 24 h after Cas9 induction, U2OS cells expressing sgRNA ctrl or E4F1 were stained with γ H2AX (red). Representative images (Left) and quantification (Right) are depicted. $n = 2$. Median in red, Mann-Whitney U test. Nuclei are counterstained with DAPI (blue). (G) Dot plot and median (red) of the quantification of spontaneous γ H2AX foci number in U2OS nuclei at 72 h after infection with control or E4F1 shRNAs. $n = 3$, Mann-Whitney U test. (H) Dot plot and median (red) of γ H2AX foci number in U2OS nuclei not treated (NT) or exposed to CPT (1 μ M, 20 min) with a 1- to 8-h recovery period. Cells were infected with control or E4F1 shRNAs at 72 h before the experiment, $n = 2$, Mann-Whitney U test. (I) Dot plot and median (red) of γ H2AX foci number in U2OS nuclei not treated (NT) or exposed to 10 Gy γ -irradiation with a 1- to 8-h recovery period. Cells were infected with control or E4F1 shRNAs at 72 h before the experiment. $n = 2$, Mann-Whitney U test.

cellular stress (Fig. 1A). Due to the critical function of E4F1, shRNAs were preferentially used over sgRNA/Cas9 for further investigations. Indeed, the effects on proliferation and cell cycle progression were more modest (SI Appendix, Fig. S1 B–E), particularly at early time points (within 96 h), which allowed investigation of DDR-associated phenotypes when apoptosis/necrosis was not yet detected. Under these conditions, RNA-sequencing analyses of *E4F1*-depleted U2OS cells revealed strong up-regulation of E2F targets and G2/M checkpoint genes in accordance with known cell cycle-related functions of E4F1 (Fig. 1D and E and SI Appendix, Fig. S2A and Table S1). Gene Set Enrichment Analysis (GSEA) also pointed to the up-regulation of DNA replication and DNA repair-related pathways (Fanconi, ATR response to replicative stress, and DSB) after *E4F1* down-regulation. Importantly, we observed an increased number of spontaneous γ H2AX foci in *E4F1*-depleted cells, whether using CRISPR-Cas9 methodology (Fig. 1F) or, less importantly but still significantly, with shRNAs (Fig. 1G). Phospho-ATM, which more specifically marks DSBs, was also increased in *E4F1*-depleted cells (SI Appendix, Fig. S2B). In addition, delayed γ H2AX foci clearance was observed in *E4F1* down-regulated cells after exposure to camptothecin (CPT) or γ -irradiation (Fig. 1H and I). These results are indicative of a DNA repair defect in *E4F1*-depleted cells.

Our group and others previously reported that *E4F1* loss strongly reduced CHK1 protein levels in murine cells (5, 12). However, *E4F1* depletion by shRNA or CRISPR-Cas9 approaches in the U2OS cell line is concomitant with a modest reduction of CHK1 protein and mRNA levels (Fig. 1A and SI Appendix, Figs. S1B and S2C). As expected, CHK1 loss impaired cell survival and proliferation of U2OS cells (Fig. 1B) but with a distinct phenotype compared with that found in *E4F1*-deleted cells. Indeed, *Chk1*-deficient cells accumulate in mitosis; in contrast, *E4F1*-null cells arrest in G2 phase (Fig. 1C). In addition, ectopic expression of CHK1 in *E4F1*-depleted cells was not able to rescue those cells (SI Appendix, Fig. S2D and E), indicating that the observed *E4F1* phenotypes in human cells are not fully related to the alteration in CHK1 protein level.

E4F1 Is Rapidly Recruited to DNA Lesions. Immunofluorescence experiments showed a partial colocalization of E4F1 with γ H2AX as well as phospho-ATM foci, both in nontreated cells and in cells subjected to genotoxic insults following exposure to CPT or γ -irradiation (Fig. 2A and SI Appendix, Fig. S3A and B). *E4F1*-null cells were used to validate the specific foci staining of the antibody (SI Appendix, Fig. S2B). A laser microirradiation recruitment assay also showed relocation of E4F1 concomitant with γ H2AX at the site of DNA damage (Fig. 2B). In addition, a proximity ligation assay (PLA) revealed a close proximity between endogenous E4F1 and ATR in nontreated cells that is further enhanced after exposure to the DNA replication inhibitor hydroxyurea (HU) (Fig. 2C and SI Appendix, Fig. S3C). To further confirm these observations, we generated a functional GFP-E4F1 fusion protein (SI Appendix, Fig. S3D and E) that also showed partial colocalization with phospho-ATM foci in nontreated, γ -irradiated, or CPT-treated U2OS cells (Fig. 2D). Microirradiation experiments showed that this GFP-E4F1 is actively recruited within minutes to laser-induced DNA lesions (Fig. 2E). Using the Cdt1-RFP cell cycle reporter (13), we also determined that GFP-E4F1 recruitment is independent of cell cycle phase (SI Appendix, Fig. S3F).

E4F1 Is Recruited to DNA Lesions through PARP-1 Activity. We then used chemical inhibitors of major DDR effectors to assess the mechanisms involved in E4F1 recruitment to DNA lesions. ATM, ATR, or dual ATM/ATR inhibitors had no impact on the kinetics of GFP-E4F1 recruitment at laser-induced DNA damage sites (SI Appendix, Fig. S4A). Strikingly, inhibition of poly(ADP ribose) polymerase 1 (PARP-1) using four different compounds completely

abrogated GFP-E4F1 recruitment (Fig. 3A; ratio of fluorescence between the damaged region and control region remains at 1). This was further confirmed using *PARP-1*-deficient HEK 293T cells (Fig. 3B) in which GFP-E4F1 could not preferentially accumulate to induce DNA lesions.

E4F1 coimmunoprecipitation (co-IP) experiments showed interactions with PARP-1 and the poly(ADP ribose) (PAR) polymer, whose synthesis is severely reduced in *PARP-1*-deficient HEK 293T cells (Fig. 3C). However, no interaction could be detected in vitro between E4F1 and PARP-1 recombinant proteins (Fig. 3D), suggesting an indirect physical interaction between the two proteins. We thus asked whether PAR could bridge the interaction between E4F1 and PARP-1, given that PAR acts as a loading platform for the recruitment of numerous DDR proteins, including ZnFs. Purified recombinant E4F1 was slot-blotted onto a nitrocellulose membrane and tested for its ability to bind 32 P-labeled PAR (Fig. 3E). Indeed, E4F1 showed a strong affinity for PAR polymer in vitro.

The addition of PAR chains along the chromatin as a consequence of PARP-1 activation also constitutes a strong driving force in chromatin decondensation. In 2019, Huet et al. (14) showed that proteins containing DNA-binding domains could be recruited to DNA lesions after PAR-dependent chromatin opening. In line with this, we observed that mutational disruption of the two first ZnF domains of E4F1 that impaired chromatin binding (Fig. 3F) also reduced its recruitment to laser tracks (Fig. 3G). As a control, we did not observe a difference in the association with DNA for a GFP-E4F1 variant lacking the E3 ligase domain. In addition, *HPF1* depletion, which regulates PARP-1 ADP ribosylation activity (15), impaired GFP-E4F1 recruitment and retention to laser-induced DNA damage sites (SI Appendix, Fig. S4B).

Our results thus suggest that both PAR-binding and ZnF DNA-binding domains of E4F1 could be at play in its recruitment to DNA damage sites.

E4F1 Promotes DNA-End Resection and HR. Since E4F1 is recruited to DNA breaks, and knowing its interplay with CHK1 protein, we monitored DDR signaling in response to genotoxic insults. After γ -irradiation exposure, we observed delayed phosphorylation of CHK1 and CHK2 signaling proteins in *E4F1*-depleted cells (Fig. 4A and SI Appendix, Fig. S5A). CHK1 phosphorylation at Ser345 was also attenuated and delayed following CPT- or HU-induced replication stress (Fig. 4B and C). This can result from down-regulation of the global CHK1 protein levels observed in *E4F1*-depleted cells and/or a lack of proper ATR activation on DNA damage. ATR activation is triggered by RPA-coated ssDNA regions generated through DNA-end resection and is predominant during S phase.

To determine whether E4F1 acts on DNA-end resection, we monitored ssDNA generation following CPT treatment by a BrdU incorporation assay. We observed significant decreases in the number and intensity of BrdU foci in S phase *E4F1*-depleted cells (Fig. 4D and SI Appendix, Fig. S5B), indicative of a defect in DNA-end resection. In addition, we monitored the accumulation of RPA that binds to ssDNA to promote HR. Our results show that *E4F1* depletion reduces the accumulation of phospho-RPA in CPT-treated cells, while total RPA protein level was not affected (Fig. 4C). Accordingly, the number of foci and intensity of phospho-RPA staining were reduced in *E4F1*-depleted cells in response to replicative stress (Fig. 4E and SI Appendix, Fig. S5C). Loading of downstream effector RAD51 was also impaired in the absence of E4F1 (SI Appendix, Fig. S5D). Since DNA-end resection is critical for DNA repair by HR, we used the DR-GFP HR reporter system to monitor whether the absence of E4F1 results in a defective HR repair pathway. *E4F1* down-regulation, using two different shRNAs, showed an $\sim 50\%$ reduction in HR efficiency (Fig. 4F). Of note, levels of I-SceI nuclease were similar in all conditions, and experiments were performed at a

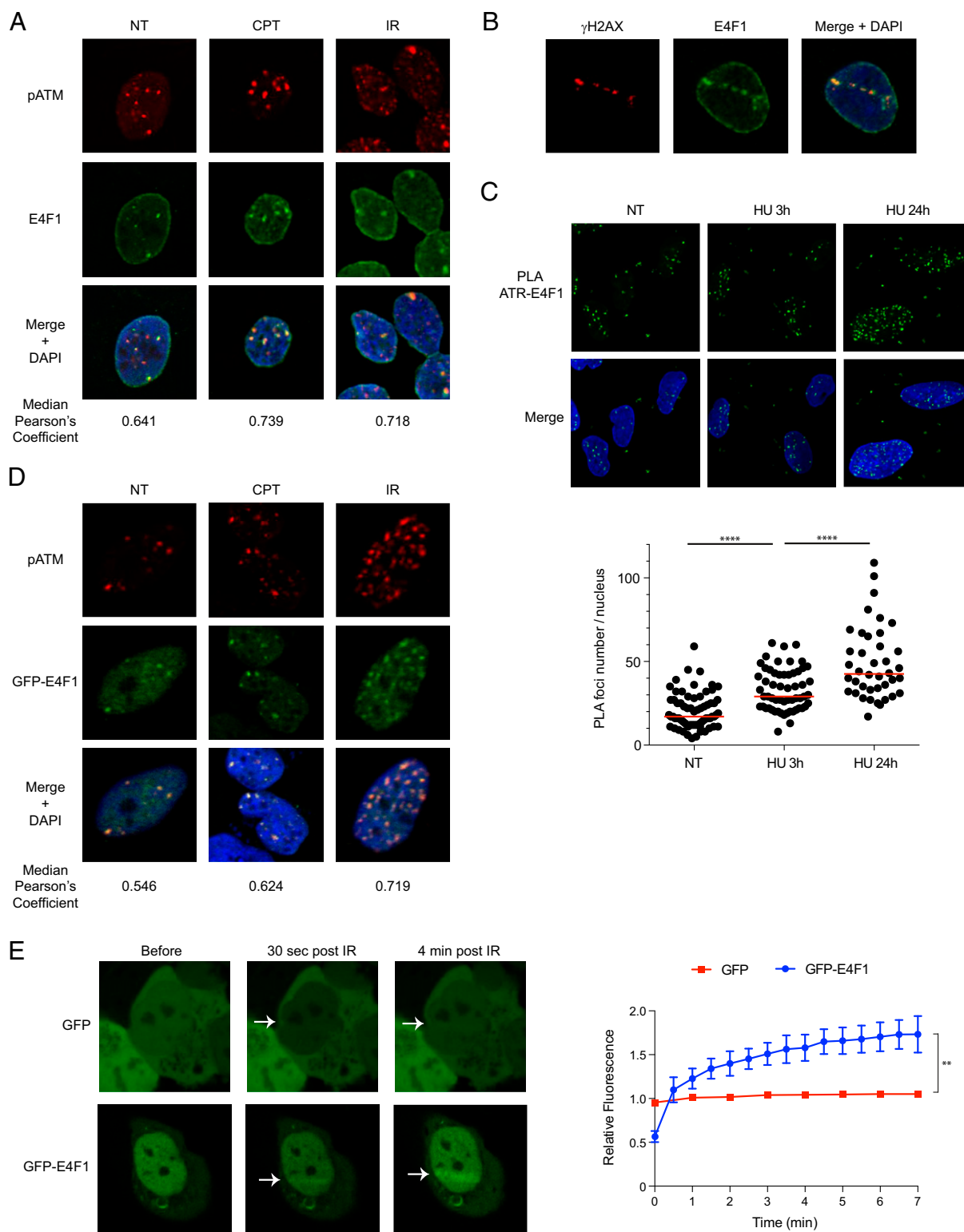


Fig. 2. E4F1 is actively recruited to DNA lesions. (A) Immunostaining of E4F1 (green) and pATM (red) in nontreated (NT) U2OS cells or after exposure to 1 μ M CPT or 10 Gy ionizing radiation (IR). Colocalized foci appear in yellow in merge panels, and nuclei are counterstained with DAPI (blue). (B) Immunostaining of E4F1 (green) and γ H2AX (red) at 30 min after laser-induced DNA damage in U2OS cells. Colocalized foci appear in yellow in merge panels, and nuclei are counterstained with DAPI (blue). (C) U2OS cells treated with HU (2 mM, for 3 h or 24 h) or not treated (NT) were fixed and processed for a PLA using anti-E4F1 and anti-ATR antibodies. Representative images (Top) and quantification (Bottom) of the number of PLA foci (green) per nucleus are presented. $n = 2$, median in red, Mann-Whitney U test. Nuclei are counterstained with DAPI (blue). (D) Immunostaining of pATM (red) in U2OS cells expressing the GFP-E4F1 fusion protein (green). Cells were exposed to 1 μ M CPT or 10 Gy IR or left untreated (NT). Colocalized foci appear in yellow in merge panels and nuclei are counterstained with DAPI (blue). (E) Live GFP and GFP-E4F1 fusion protein recruitment to laser-induced DNA lesions in U2OS cells. Representative pictures taken before and at 30 s and 4 min after microirradiation (Left) and quantification over time (Right); Mann-Whitney U test. Error bars represent mean \pm SD. (A and D) Median Pearson's coefficient was calculated using the colocalization plugin JACoP from ImageJ software.

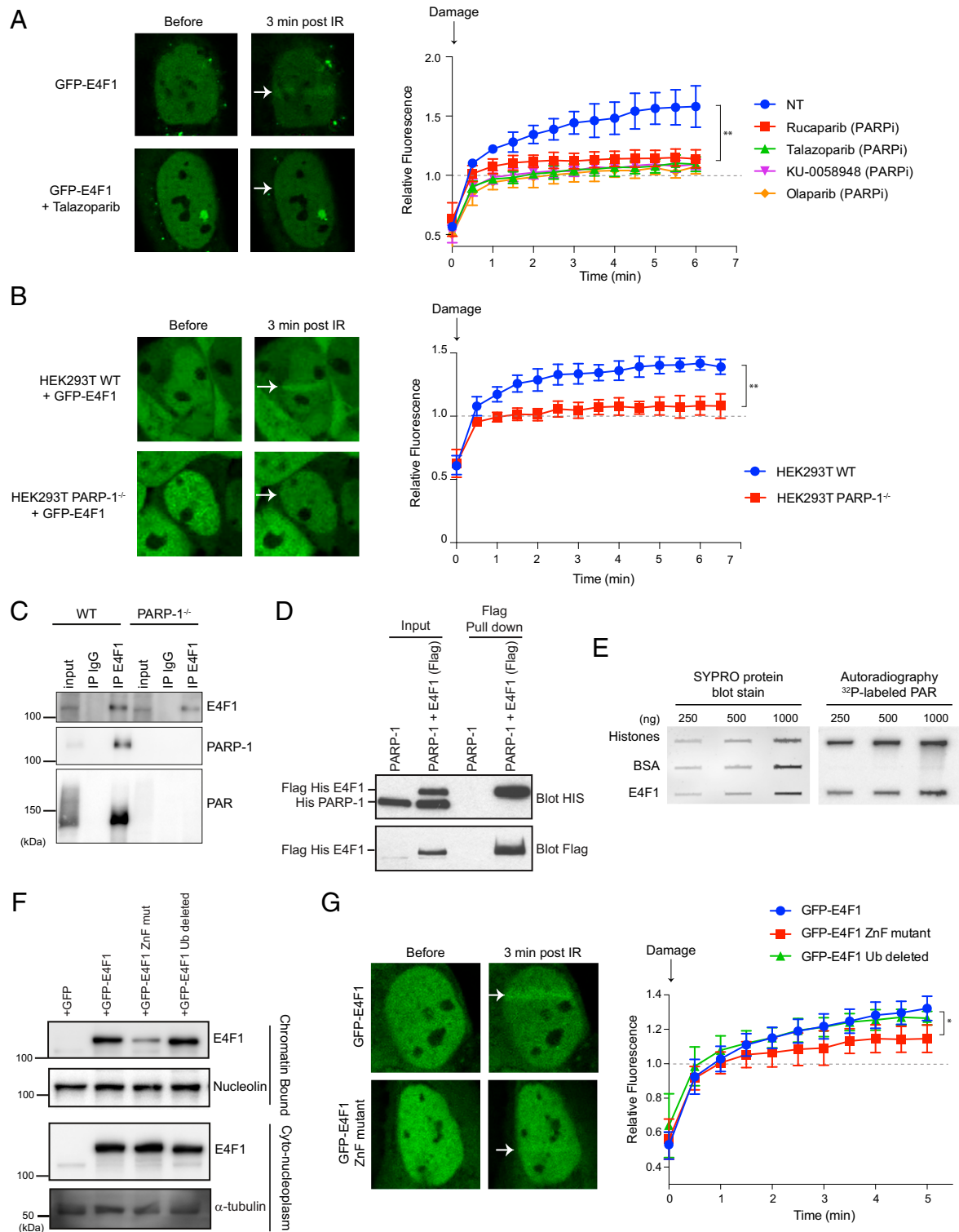


Fig. 3. E4F1 recruitment to DNA damage is PARP-1–dependent. (A) Quantification (Right; Mann–Whitney U test) of live GFP-E4F1 fusion protein recruitment to laser-induced DNA lesions in nontreated (NT) U2OS cells or after exposure to PARP inhibitors. (Left) Representative pictures taken before and 3 min after microirradiation. (B) Quantification (Right; Mann–Whitney U test) of live GFP-E4F1 fusion protein recruitment to laser-induced DNA lesions in HEK 293T WT and *PARP-1*–deficient cells. (Left) Representative pictures taken before and 3 min after microirradiation. (C) E4F1 co-IP experiment performed on total cell extracts from HEK 293T WT and *PARP-1*–deficient cells. Normal mouse IgG served as a negative control. (D) Result of in vitro co-IP assay using purified Flag-His-E4F1 and His-PARP-1 proteins. (E) PAR-binding assay measuring binding of 32 P-labeled PAR polymer to increasing amounts of purified E4F1 protein (Right). Bovine serum albumin (BSA) and purified histones served as negative and positive controls, respectively. SYPRO protein blot stain served as a loading control (Left). (F) HEK293 cells were infected to express control GFP, WT GFP-E4F1, and GFP-E4F1 carrying mutations in its two first ZnFs or GFP-E4F1 depleted for its E3 ligase domain. Chromatin-bound and cytonucleoplasm protein fractions were isolated and loaded for immunoblotting against E4F1. Nucleolin and α -tubulin served as loading controls. (G) Quantification of live WT and mutated GFP-E4F1 fusion protein recruitment to laser-induced DNA lesions in U2OS cells (Right) and representative pictures taken before and at 3 min after microirradiation (Left). In A, B, and G, error bars represent mean \pm SD.

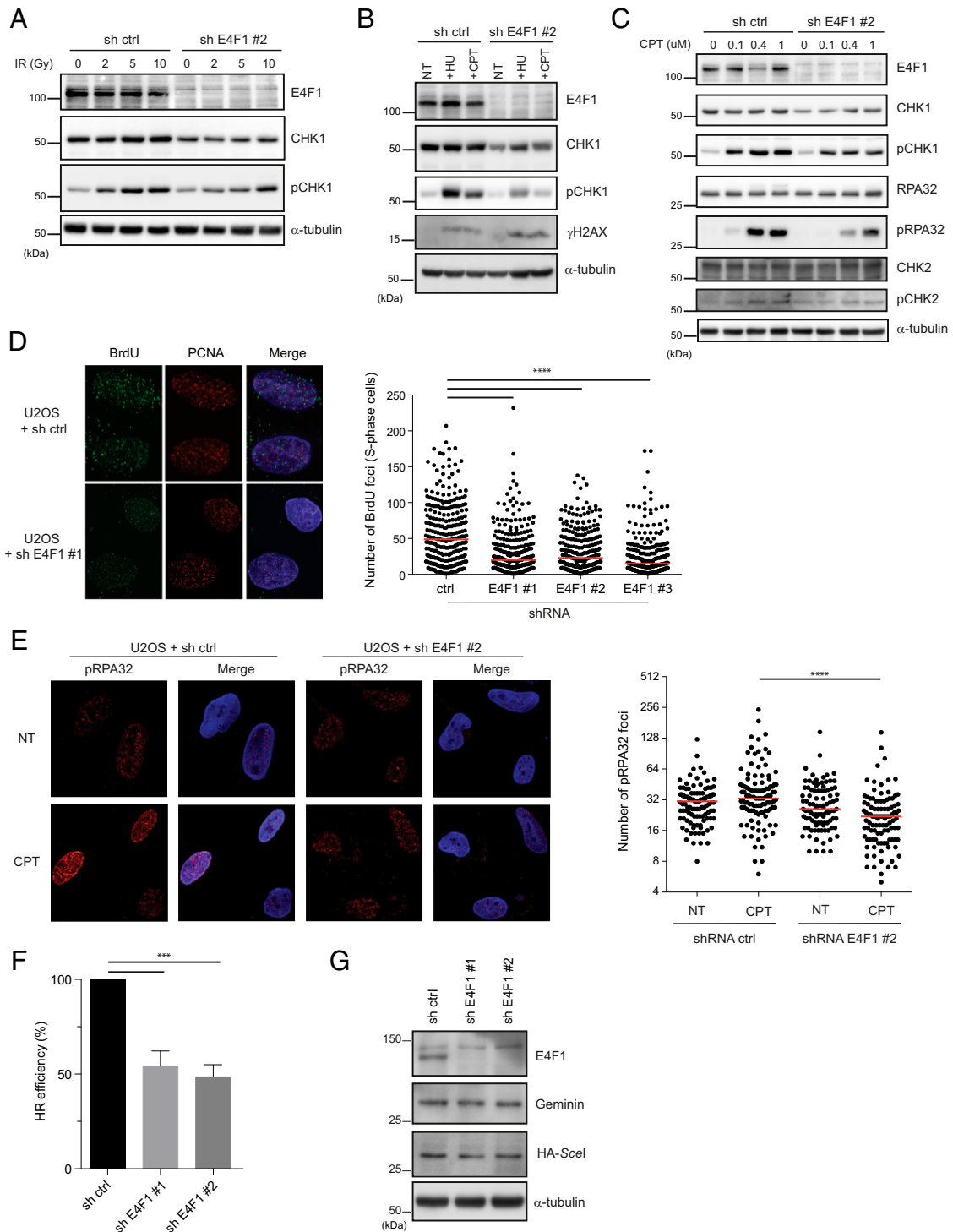


Fig. 4. E4F1 promotes DNA-end resection and HR. (A) Immunoblot of total E4F1, CHK1, and p-CHK1 (ser345) proteins in U2OS cells infected with the indicated shRNAs for 72 h. Before analysis, cells were treated with increasing amounts of IR (0 to 10 Gy) and released for 1 h. α -tubulin served as a loading control. (B) Immunoblot of total E4F1, CHK1, p-CHK1 (ser345), and γ H2AX proteins in U2OS cells infected with indicated shRNAs for 72 h. Before analysis, cells were treated for 1 h with CPT (1 μ M) or HU (2 mM) or left untreated (NT). α -tubulin served as a loading control. (C) Immunoblot of total E4F1, CHK1, p-CHK1 (ser345), RPA32, p-RPA32 (S4/S8), CHK2, and p-CHK2 (Thr68) proteins in U2OS cells infected with indicated shRNAs for 72 h. Before analysis, cells were treated 1 h with increasing amounts of CPT (0 to 1 μ M). α -tubulin served as a loading control. (D) U2OS cells infected with indicated shRNAs were treated with CPT (1 μ M, 1 h), followed by a 1-h release. Cells were then subjected to immunofluorescence against BrdU and PCNA (Left), and nuclei were counterstained with DAPI (blue). The BrdU foci were quantified in PCNA-positive cells (Right). $n = 3$. Medians are in red, Mann-Whitney U test. (E) Representative immunostainings (Left) of p-RPA32 (S4/S8) in U2OS cells infected with indicated shRNAs for 72 h. Before analysis, cells were treated for 1 h with CPT (1 μ M) or left untreated (NT). Nuclei were counterstained with DAPI (blue). The foci of p-RPA32 were quantified in each nucleus (Right). $n = 2$. Medians in red, Mann-Whitney U test. (F) HR efficiency was assessed by quantification of U2OS GFP-positive cells at 48 h after transfection with the DR-GFP plasmids. Cells were previously infected with indicated shRNAs, and results were normalized as efficiency in shRNA control is equal to 100%. $n = 3$, t test. (G) Immunoblot of total E4F1, Geminin, and HA-SceI proteins in U2OS cells used to monitor HR efficiency from (F). α -tubulin served as a loading control.

time when no major differences in cell cycle profiles were observed (Fig. 4G). Protein levels of DNA-end resection and HR repair factors, such as RPA, RAD51, BRCA2, and FANCD2, were not reduced after *E4F1* depletion (SI Appendix, Fig. S5E).

E4F1 Is Required for Transcriptional Silencing at DSBs. To further dissect the role of E4F1 at DSBs, we used the U2OS-*FokI* reporter system that enables visualization of DSB repair protein recruitment as well as transcription in *cis* (16). As was observed for γ H2AX and pCHK1, we showed that E4F1 colocalized with mCherry-*FokI* endonuclease at the site of DSBs (Fig. 5A and B). PLA also revealed a specific interaction, or very close proximity, between E4F1 and activated phospho-ATM at DSB sites (Fig. 5C). On the other hand, nuclease-deficient D450A *FokI* failed to recruit E4F1 and to induce a PLA signal between E4F1 and activated pATM (Fig. 5A–C), demonstrating that E4F1 is specifically recruited to injured DNA in this reporter system. In addition, and due to transcriptional silencing following DNA damage, the active phospho-Ser2 RNA polymerase is excluded from *FokI* foci while still present in control cells expressing the nuclease-deficient D450A *FokI* (Fig. 5A and B). In this reporter system, a YFP-MS2 RNA is transcribed on the addition of doxycycline and allows monitoring of transcription at the site of *FokI*-induced DSBs. The loss of YFP-MS2 signal at *FokI* foci reflects the ongoing transcriptional silencing compared to its accumulation when DNA is not altered by the *FokI* mutant. Importantly, loss of E4F1 in these cells efficiently abolished the transcriptional silencing at *FokI*-induced DSBs (Fig. 5D). ATM inhibition, which is known to abrogate transcriptional shutdown at injured DNA, was used as a positive control. Together, these results demonstrate steady E4F1 recruitment at induced DSBs and its role in subsequent transcriptional silencing.

E4F1 Recruits BRG1 to DNA Lesions. Our findings involving E4F1 in DNA damage-associated transcriptional silencing is reminiscent of the chromatin remodeling that occurs in the first steps of DNA repair (17). We thus tested the recruitment of several chromatin remodeling factors in *E4F1*-depleted cells and found that E4F1 is required for the proper recruitment of GFP-BRG1 (Fig. 6A). Immunoblotting of chromatin-bound fraction also showed an E4F1-dependent BRG1 enrichment at chromatin after CPT exposure (Fig. 6B). BRG1 physically interacts with PARP-1 (18) and acts as the ATPase subunit of the mammalian SWI/SNF chromatin remodeling complex and has been involved in DNA repair (17, 19, 20). Similar to E4F1, we showed that BRG1 recruitment to DNA lesions is PARP-1-dependent as talazoparib treatment completely abolished GFP-BRG1 enrichment at laser tracks (Fig. 6C). On the other hand, BRG1 depletion did not impact GFP-E4F1 recruitment (SI Appendix, Fig. S6A), indicating that E4F1 is recruited independently of BRG1.

Interestingly, *in vitro* pull-down assays with the two recombinant proteins indicated that E4F1 and BRG1 could interact directly (Fig. 6D). Co-IP in cellular extracts, either nontreated or exposed to genotoxic agents, revealed an interaction between E4F1 and BRG1 (Fig. 6E). We noticed that co-IP was increased after CPT treatment compared to nontreated or irradiated cells. This could indicate that the E4F1–BRG1 interaction is promoted depending on the type of DNA lesions, which is concomitant with the observation that BRG1 is more efficiently recruited to chromatin after CPT treatment than after γ -irradiation (Fig. 6F). BAF60a, another member of the mammalian SWI/SNF complex, follows a similar pattern as that of BRG1 in its interaction with E4F1.

As reported previously (20), *BRG1* knockdown decreases HR efficiency in the DR-GFP HR reporter system (SI Appendix, Fig. S6B and C). Interestingly, codepletion of *E4F1* and *BRG1* did not result in further reductions in HR efficiency compared to *E4F1*-only depletion (Fig. 6G), supporting a model in which these proteins work within the same DNA repair pathway. Of

note, levels of I-*SceI* nuclease were similar in all conditions (Fig. 6H), and experiments were performed at a timepoint when no major differences in cell cycle profiles could be observed (SI Appendix, Fig. S6D). Importantly, *E4F1* depletion did not cause any significant changes in the total BRG1 mRNA and protein levels (SI Appendix, Fig. S6E and F). Together, these data suggest that E4F1 is involved in the PAR-assisted recruitment of a specific SWI/SNF subcomplex, including BRG1, at damaged chromatin.

E4F1 Is Amplified and Overexpressed in a Subset of Human Breast Cancer. In the light of these results, we investigated *E4F1* expression levels in the DepMap human cancer collection and found that while *E4F1* is ubiquitously expressed, breast cancers are among the highest expressors (SI Appendix, Fig. S7A). In The Cancer Genome Atlas (TCGA) database (21, 22), we also noted that an unappreciated proportion of breast cancers includes *E4F1* alterations, predominantly gene amplifications or missense mutations (Fig. 7A). Indeed, breast cancers and invasive breast carcinomas from two different cohorts (METABRIC and TCGA) showed the greatest number of alterations, with 160 (7.36%) and 45 (4.15%) cases of *E4F1* gene amplification reported, respectively. Importantly, gene amplification was associated with higher *E4F1* mRNA levels (Fig. 7B and SI Appendix, Fig. S7B). These tumors were mostly estrogen receptor (ER)-positive and HER2-negative and presented mostly as grade 2 tumors (SI Appendix, Fig. S7C). Most intriguingly, *E4F1* amplification, which is at least as frequent as *BRCA1* and *BRCA2* alterations, appeared to be mostly mutually exclusive of these anomalies (Fig. 7C). While *E4F1* expression showed no impact on the survival of low-grade breast cancer patients, Kaplan–Meier plot analysis (23) revealed that grade 3 breast cancer patients with higher *E4F1* expression had significantly worse survival probability compared with patients with lower *E4F1* levels ($P = 0.0018$) (SI Appendix, Fig. S7D). As seen with *E4F1*, *BRG1* (*SMARCA4*) is also amplified and overexpressed in a small proportion of human breast cancers and appears to be mutually exclusive of *E4F1* and *BRCA1/2* alterations (SI Appendix, Fig. S7E).

Discussion

In this report, we describe a molecular mechanism that establishes E4F1 as a DNA damage protein involved in DSB repair. Looking at endogenous and GFP-tagged E4F1 protein, we determined that E4F1 is rapidly recruited to DNA lesions through PARP-1 activity. Moreover, we documented that E4F1 promotes DNA-end resection and HR and is required for transcriptional silencing at DSB, likely through its interaction with BRG1.

Chromatin remodeling is one of the first events occurring in the DNA repair process that overcomes the barrier of condensed chromatin and ensures accessibility to DNA repair factors (24–27). In particular, the mammalian ATP-dependent complex SWI/SNF participates in DSB repair by promoting H2AX phosphorylation at Ser-139 (γ H2AX) (28, 29), activating the ATR/CHK1 pathway (30), loading of RAD51 (20, 31), and ensuring proper transcriptional silencing (32). Interestingly, these features are reminiscent of what we have linked to E4F1 function. Notably, we have shown that E4F1 interacts with BRG1 and is required for its recruitment to laser-induced DNA lesions. This suggests that at least some of the phenotypes associated with *E4F1* loss are related to defective BRG1 engagement to DNA repair. As for E4F1, we reported that BRG1 recruitment requires PARP-1 activity. Accordingly, BRG1 and other SWI/SNF members have been previously identified as PAR-associated proteins by systematic proteomic studies (33, 34). Taken together, these results suggest that PARP-1, E4F1, and BRG1 cooperate in DNA repair.

Within seconds following DNA damage, a massive amount of PAR is synthesized, mainly by PARP-1, and acts as a recruitment platform for DDR proteins (35, 36). Importantly, local accumulation

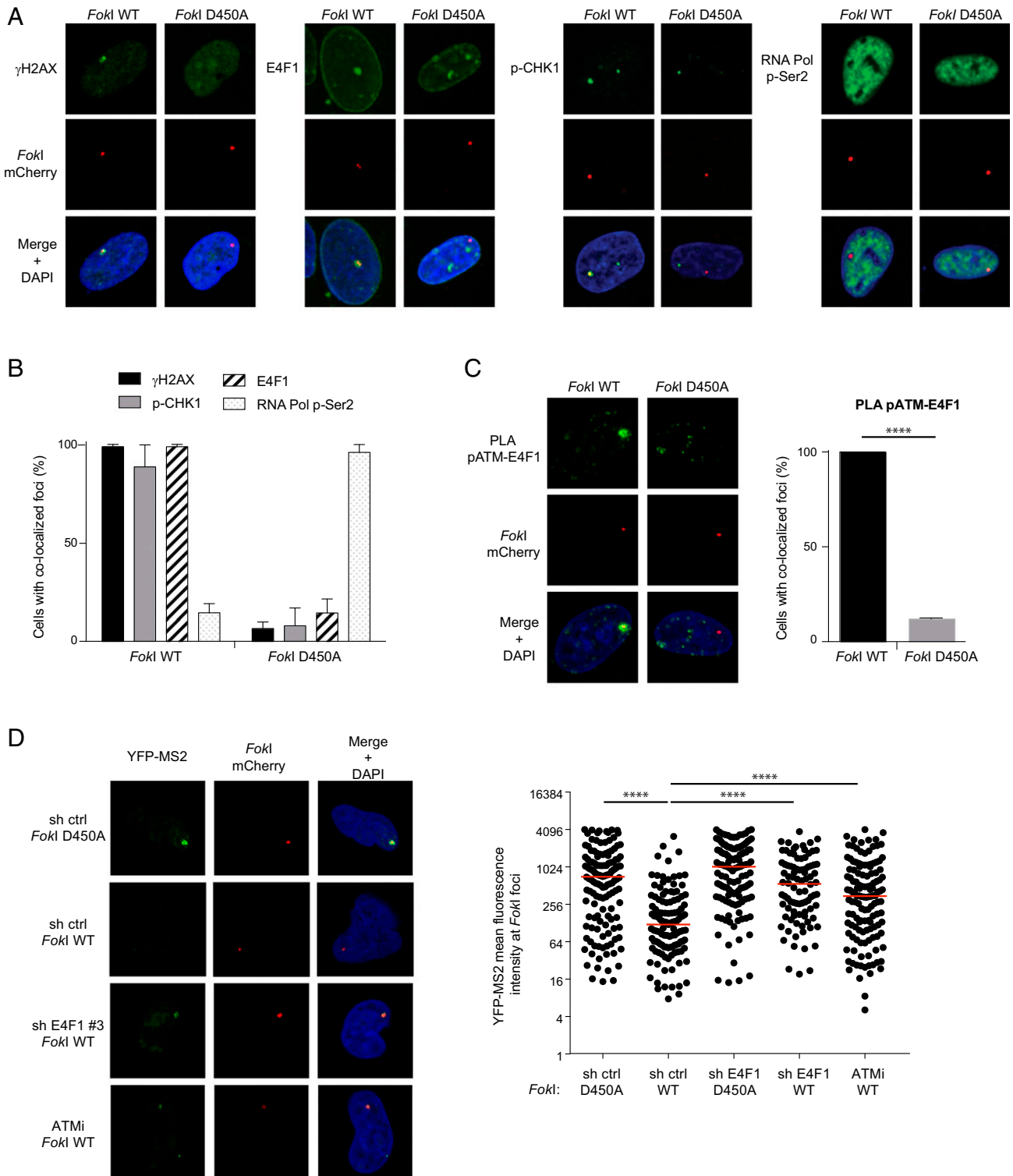


Fig. 5. E4F1 is recruited to induced DSBs and is required for transcriptional silencing. (A) U2OS-*LacI-FokI-mCherry* DSB reporter cells were infected with lentiviruses expressing WT or catalytic-deficient D450A *mCherry-FokI* constructs for 48 h before fixation and stained for γ H2AX, E4F1, p-CHK1, or actively elongating RNA Pol II phospho-Ser2 (green). Representative images are depicted. (B) Quantification ($n = 3$) of the percentage of cells presenting a colocalization signal between the *mCherry-FokI* foci and green immunofluorescence from A. (C) U2OS-*LacI-FokI-mCherry* reporter cells were infected with lentiviruses expressing WT or catalytic-deficient D450A *mCherry-FokI* constructs for 48 h before fixation and then processed for PLA (green signal) using anti-pATM and anti-E4F1 antibodies (Left). Quantification of the percentage of cells presenting a PLA signal at *mCherry-FokI* foci (Right). $n = 3$, t test. Error bars represent mean with SD. (D) U2OS-*LacI-FokI-mCherry* reporter cells expressing the indicated shRNA constructs were infected with lentiviruses expressing WT or catalytic-deficient D450A *mCherry-FokI* constructs for 24 h. Transcription was induced by doxycycline treatment for 5 h and visualized by the accumulation of YFP-MS2 protein at the site (green). Cells were fixed and counterstained with DAPI. Representative images are depicted (Left), and YFP-MS2 relative mean fluorescence intensity at the *FokI* foci was quantified using ImageJ software (Right). Treatment with the ATM inhibitor KU-55933 served as a positive control. $n = 3$. Medians are in red, Mann-Whitney U test.

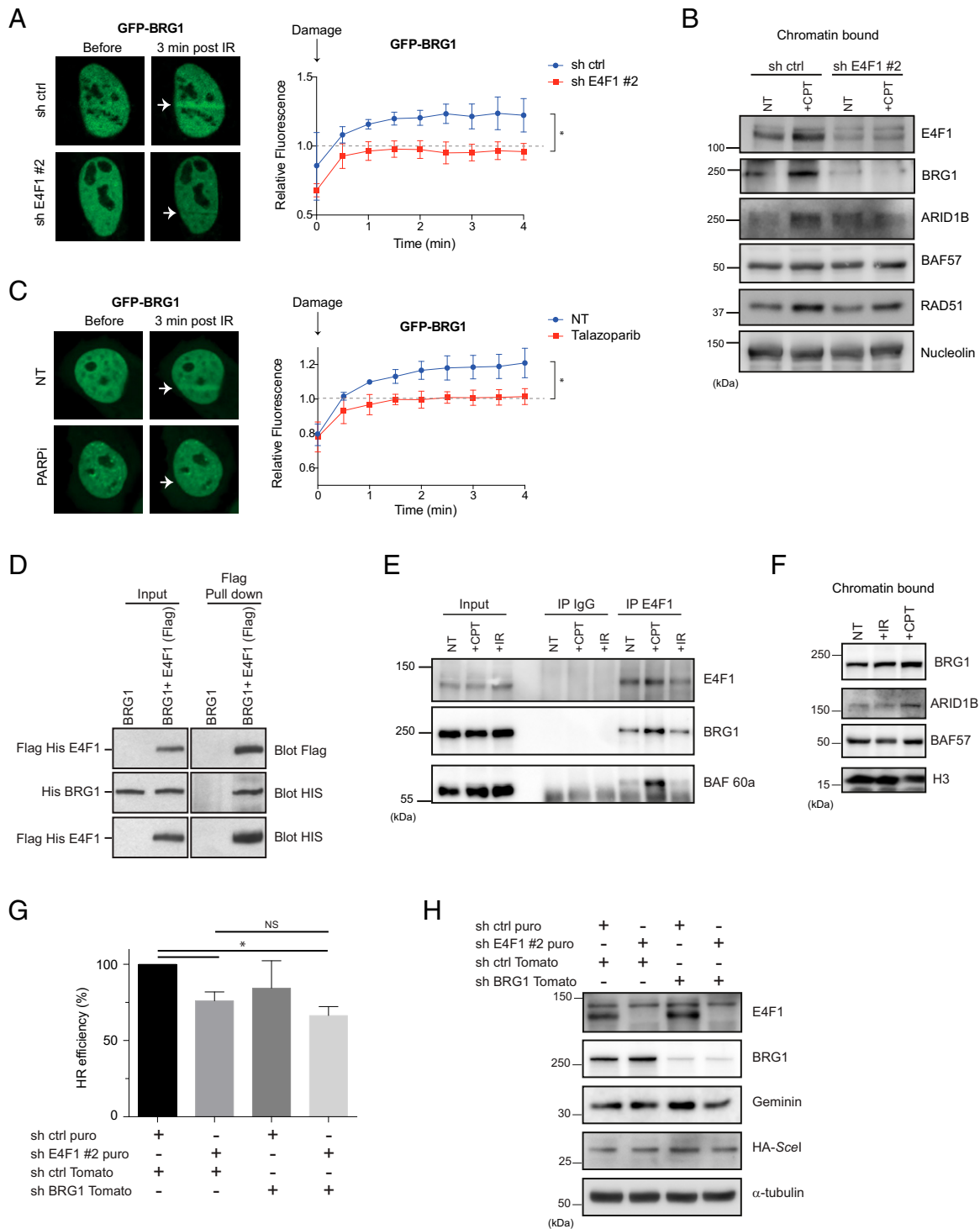


Fig. 6. E4F1 interacts and recruits BRG1 to DNA lesions. (A) Quantification (Right; Mann-Whitney *U* test) of live GFP-BRG1 fusion protein recruitment to laser-induced DNA lesions in U2OS cells infected with shRNA control or targeting *E4F1*. Representative pictures taken before and 3 min after microirradiation are shown (Left). Error bars represent mean with SD. (B) Chromatin-bound protein extraction was performed on HEK293 cells infected with corresponding shRNAs and left untreated (NT) or exposed for 1 h to CPT (1 μ M). Immunoblots were performed using indicated antibodies, and nucleolin served as a loading control. (C) Quantification (Right; Mann-Whitney *U* test) of live GFP-BRG1 fusion protein recruitment to laser-induced DNA lesions in U2OS cells treated with PARP inhibitor (talazoparib) or left untreated (NT). Representative pictures taken before and 3 min after microirradiation are depicted (Left). Error bars represent mean with SD. (D) Result of in vitro co-IP assay using purified Flag-His-E4F1 and His-BRG1 proteins. (E) E4F1 co-IP experiment performed on total cell extracts from U2OS cells. Before analysis, cells were treated for 1 h with CPT (1 μ M), exposed to IR (10 Gy) or left untreated (NT). Normal mouse IgG served as a negative control. (F) Chromatin-bound protein extraction was performed on NT HEK293 cells or following exposure to γ -irradiation (5 Gy; 1 h release) or CPT (1 μ M; 1 h). Immunoblots were performed using indicated antibodies, and H3 served as a loading control. (G) HR efficiency was assessed by quantification of U2OS GFP-positive cells at 48 h after transfection with the DR-GFP plasmids. Cells were previously coinfecting with the indicated shRNAs for 72 h. Results were normalized as efficiency in shRNA control is equal to 100%. $n = 2$, *t* test. (H) Immunoblot of total E4F1, BRG1, Geminin, and HA-SceI proteins in U2OS cells used to monitor HR efficiency from G. α -tubulin served as a loading control.

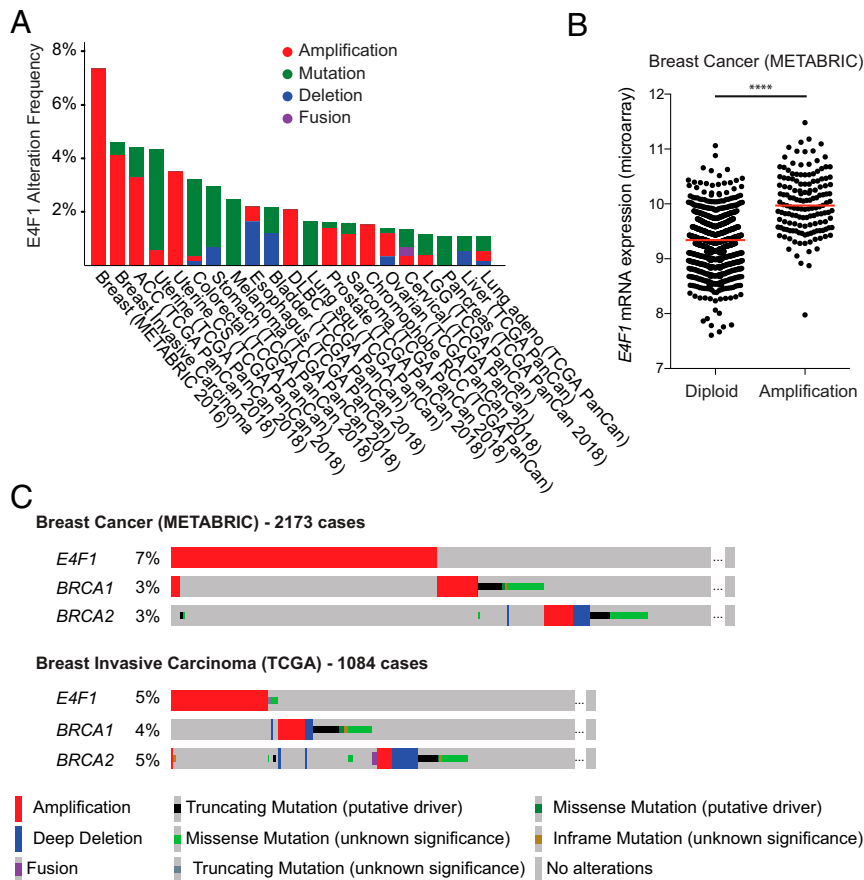


Fig. 7. *E4F1* is amplified in breast cancers and is mutually exclusive with *BRCA1/2* alterations. (A) Bar plot reporting the frequency of *E4F1* alterations (gene amplification, mutation, deletion, or fusion) in a wide range of human cancers (source: cBioPortal). (B) Dot plot of *E4F1* mRNA expression in the METABRIC (breast cancer) cohort bearing or not bearing *E4F1* gene amplification. The reference population represents all samples that are diploid for the gene of interest. Median in red, *t* test. (C) Representation of *E4F1*, *BRCA1*, and *BRCA2* alterations in the METABRIC and TCGA breast cancer cohorts (source: cBioPortal). Each vertical line represents a patient sample. The frequency of total alterations is indicated.

of PAR at DNA lesions also constitutes a driving force of chromatin decondensation. By virtue of their long-chain nature, polymers of ADP ribose alter the electrostatic charge density of lysine-rich histone proteins, which weakens histone–DNA interactions and promotes chromatin remodeling. PAR-dependent chromatin opening has been shown to be sufficient to recruit DNA-binding proteins at DNA lesions (14). The dual action of PARylation makes it particularly difficult to discriminate between the dependence of a factor’s affinity for PAR chains and increased local accessibility to chromatin for its accumulation at DNA damage sites. No consensus sequences for PAR binding have been identified in *E4F1*; however, *E4F1* contains several C2H2-type ZnFs known to have both DNA-binding and PAR-binding properties (37, 38). Thus, our experiments show that *E4F1* binds in vitro to PAR polymer, and that DNA binding contributes to its dynamics at DNA lesions.

Interestingly, the E2F1-pRB complex also has been involved in BRG1 recruitment to DSBs (6), and pRB is a known direct interactor with *E4F1* (2). We believe that both pRB-E2F1 and *E4F1* may be involved in BRG1 recruitment, but this process may depend on the cell cycle context, chromatin state, or DNA lesion characteristics. Interestingly, E2F1 and *E4F1* share striking similarities: they both interact with a large variety of proteins, and beyond their well-known role in cell cycle regulation, they also control some cellular metabolic functions and participate in DNA repair. It is remarkable how multifunctional these proteins are. These are not isolated cases, and other transcription factors involved in DNA repair have been reported (39). Noncanonical repair proteins, such as

ZnF proteins, are also increasingly described as DNA repair actors, particularly in the context of DSBs (8–11). One of the emerging features is that DNA-binding proteins may be largely involved in chromatin remodeling at DNA lesions to ensure DNA accessibility. The pRB-E2F1 complex has been reported to recruit GCN5 (40) or p300/CBP (41) to induce histone acetylation and chromatin relaxation depending on the type of DNA damage. ZnF ZMYND8 protein, which also contains a bromodomain, was reported to promote transcriptional repression and HR repair by recruiting the chromatin remodeling NuRD complex to DNA lesions (42).

Our hypothesis, therefore, is that *E4F1* is one of these multifunctional proteins involved in DNA repair. Its possible relevance to breast cancer tumorigenesis is intriguing, as we have shown that the *E4F1* gene is amplified in a significant proportion of human breast cancers, mostly in a *BRCA1/2* wild-type context. In summary, our data suggest a PARP1-dependent function for *E4F1* in DSB repair that, along with its key role in regulating p53 and CHK1 function, positions this gene as a central orchestrator of genotoxic stress response.

Materials and Methods

Detailed descriptions of the cell models, cell proliferation assay, chemicals and treatments, knockdown experiments, laser microirradiation, co-IP, pull-down with recombinant proteins, Western blot, flow cytometry, the DR-GFP system, immunofluorescence, PAR-binding assay, the U2OS-LacI-FokI-mCherry DSB reporter system, PLA, BrdU assay, image capture and analysis, statistical analysis, and RNA sequencing are provided in *SI Appendix, Materials and Methods*.

Data Availability. RNA sequencing data have been deposited in the Gene Expression Omnibus (GEO) database, <https://www.ncbi.nlm.nih.gov/geo> (accession no. [GSE144958](https://www.ncbi.nlm.nih.gov/geo)).

ACKNOWLEDGMENTS. We thank Julie Lessard for scientific discussion and materials; Laurent Le Cam for E4F1 constructions; Tara Macrae and Isabel Boivin for technical assistance; Christian Charbonneau, Jennifer Huber, and

Raphaëlle Lambert at the Institute for Research in Immunology and Cancer microscopy and genomic platforms. J.-Y.M. is a Canada Research Chair in DNA repair and cancer therapeutics. C.M. is recipient of a Canadian Institutes of Health Research (CIHR) fellowship (MFE-148251). This work was supported by CIHR Grants MOP-311036 (to J.-Y.M. and G.G.P.) and MOP-82814 (to G.S.) and CIHR Foundation Grants FDN388879 (to J.-Y.M.) and FDN143286 (to G.S.).

1. L. Fajas *et al.*, Cyclin A is a mediator of p120E4F-dependent cell cycle arrest in G1. *Mol. Cell. Biol.* **21**, 2956–2966 (2001).
2. L. Fajas *et al.*, pRB binds to and modulates the transrepressing activity of the E1A-regulated transcription factor p120E4F. *Proc. Natl. Acad. Sci. U.S.A.* **97**, 7738–7743 (2000).
3. L. Le Cam *et al.*, E4F1 is an atypical ubiquitin ligase that modulates p53 effector functions independently of degradation. *Cell* **127**, 775–788 (2006).
4. L. Le Cam, M. Lacroix, M. A. Ciemerych, C. Sardet, P. Sicinski, The E4F protein is required for mitotic progression during embryonic cell cycles. *Mol. Cell. Biol.* **24**, 6467–6475 (2004).
5. D. Grote *et al.*, E4F1 is a master regulator of CHK1-mediated functions. *Cell Rep.* **11**, 210–219 (2015).
6. R. Vélez-Cruz *et al.*, RB localizes to DNA double-strand breaks and promotes DNA end resection and homologous recombination through the recruitment of BRG1. *Genes Dev.* **30**, 2500–2512 (2016).
7. S. Manickavaniyaham *et al.*, The E2F1 transcription factor and RB tumor suppressor moonlight as DNA repair factors. *Cell Cycle* **19**, 2260–2269 (2020).
8. C. K. Vilas, L. E. Emery, E. L. Denchi, K. M. Miller, Caught with one's zinc fingers in the genome integrity cookie jar. *Trends Genet.* **34**, 313–325 (2018).
9. D. M. Moquin *et al.*, Localized protein biotinylation at DNA damage sites identifies ZPET, a repressor of homologous recombination. *Genes Dev.* **33**, 75–89 (2019).
10. G. Chen *et al.*, ZNF830 mediates cancer chemoresistance through promoting homologous-recombination repair. *Nucleic Acids Res.* **46**, 1266–1279 (2018).
11. J. W. C. Leung *et al.*, ZMYM3 regulates BRCA1 localization at damaged chromatin to promote DNA repair. *Genes Dev.* **31**, 260–274 (2017).
12. G. Rodier *et al.*, The transcription factor E4F1 coordinates CHK1-dependent checkpoint and mitochondrial functions. *Cell Rep.* **11**, 220–233 (2015).
13. A. Sakae-Sawano *et al.*, Visualizing spatiotemporal dynamics of multicellular cell cycle progression. *Cell* **132**, 487–498 (2008).
14. R. Smith *et al.*, Poly(ADP-ribose)-dependent chromatin unfolding facilitates the association of DNA-binding proteins with DNA at sites of damage. *Nucleic Acids Res.* **47**, 11250–11267 (2019).
15. I. Gibbs-Seymour, P. Fontana, J. G. M. Rack, I. Ahel, HPF1/C4orf27 is a PARP-1-interacting protein that regulates PARP-1 ADP-ribosylation activity. *Mol. Cell* **62**, 432–442 (2016).
16. N. M. Shanbhag, I. U. Rafalska-Metcalf, C. Balane-Bolivar, S. M. Janicki, R. A. Greenberg, ATM-dependent chromatin changes silence transcription in cis to DNA double-strand breaks. *Cell* **141**, 970–981 (2010).
17. A. Kakarougkas, J. A. Downs, P. A. Jeggo, The PBAF chromatin remodeling complex represses transcription and promotes rapid repair at DNA double-strand breaks. *Mol. Cell. Oncol.* **2**, e970072 (2015).
18. C. T. Hang *et al.*, Chromatin regulation by Brg1 underlies heart muscle development and disease. *Nature* **466**, 62–67 (2010).
19. S.-J. Kwon *et al.*, ATM-mediated phosphorylation of the chromatin remodeling enzyme BRG1 modulates DNA double-strand break repair. *Oncogene* **34**, 303–313 (2015).
20. W. Qi *et al.*, BRG1 promotes the repair of DNA double-strand breaks by facilitating the replacement of RPA with RAD51. *J. Cell Sci.* **128**, 317–330 (2015).
21. J. Gao *et al.*, Integrative analysis of complex cancer genomics and clinical profiles using the cBioPortal. *Sci. Signal.* **6**, pl1 (2013).
22. E. Cerami *et al.*, The cBio cancer genomics portal: An open platform for exploring multidimensional cancer genomics data. *Cancer Discov.* **2**, 401–404 (2012).
23. B. Györfy *et al.*, An online survival analysis tool to rapidly assess the effect of 22,277 genes on breast cancer prognosis using microarray data of 1,809 patients. *Breast Cancer Res. Treat.* **123**, 725–731 (2010).
24. S. Allard, J.-Y. Masson, J. Côté, Chromatin remodeling and the maintenance of genome integrity. *Biochim. Biophys. Acta* **1677**, 158–164 (2004).
25. Y. Bao, X. Shen, Chromatin remodeling in DNA double-strand break repair. *Curr. Opin. Genet. Dev.* **17**, 126–131 (2007).
26. J. A. Downs, M. C. Nussenzweig, A. Nussenzweig, Chromatin dynamics and the preservation of genetic information. *Nature* **447**, 951–958 (2007).
27. H. van Attikum, S. M. Gasser, Crosstalk between histone modifications during the DNA damage response. *Trends Cell Biol.* **19**, 207–217 (2009).
28. J.-H. Park *et al.*, Mammalian SWI/SNF complexes facilitate DNA double-strand break repair by promoting gamma-H2AX induction. *EMBO J.* **25**, 3986–3997 (2006).
29. H.-S. Lee, J.-H. Park, S.-J. Kim, S.-J. Kwon, J. Kwon, A cooperative activation loop among SWI/SNF, gamma-H2AX and H3 acetylation for DNA double-strand break repair. *EMBO J.* **29**, 1434–1445 (2010).
30. S. L. Smith-Roe *et al.*, SWI/SNF complexes are required for full activation of the DNA-damage response. *Oncotarget* **6**, 732–745 (2015).
31. G. Peng *et al.*, BRIT1/MCPH1 links chromatin remodelling to DNA damage response. *Nat. Cell Biol.* **11**, 865–872 (2009).
32. A. Kakarougkas *et al.*, Requirement for PBAF in transcriptional repression and repair at DNA breaks in actively transcribed regions of chromatin. *Mol. Cell* **55**, 723–732 (2014).
33. J.-P. Gagné *et al.*, Quantitative proteomics profiling of the poly(ADP-ribose)-related response to genotoxic stress. *Nucleic Acids Res.* **40**, 7788–7805 (2012).
34. D. M. Chou *et al.*, A chromatin localization screen reveals poly(ADP-ribose)-regulated recruitment of the repressive polycomb and NuRD complexes to sites of DNA damage. *Proc. Natl. Acad. Sci. U.S.A.* **107**, 18475–18480 (2010).
35. D. D'Amours, S. Desnoyers, I. D'Silva, G. G. Poirier, Poly(ADP-ribosylation) reactions in the regulation of nuclear functions. *Biochem. J.* **342**, 249–268 (1999).
36. M. Y. Kim, T. Zhang, W. L. Kraus, Poly(ADP-ribosylation) by PARP-1: “PAR-laying” NAD⁺ into a nuclear signal. *Genes Dev.* **19**, 1951–1967 (2005).
37. I. Ahel *et al.*, Poly(ADP-ribose)-binding zinc finger motifs in DNA repair/checkpoint proteins. *Nature* **451**, 81–85 (2008).
38. M. Li, L. Y. Lu, C. Y. Yang, S. Wang, X. Yu, The FHA and BRCT domains recognize ADP-ribosylation during DNA damage response. *Genes Dev.* **27**, 1752–1768 (2013).
39. L. Izhar *et al.*, A systematic analysis of factors localized to damaged chromatin reveals PARP-dependent recruitment of transcription factors. *Cell Rep.* **11**, 1486–1500 (2015).
40. R. Guo, J. Chen, D. L. Mitchell, D. G. Johnson, GCN5 and E2F1 stimulate nucleotide excision repair by promoting H3K9 acetylation at sites of damage. *Nucleic Acids Res.* **39**, 1390–1397 (2011).
41. S. Manickavaniyaham *et al.*, E2F1 acetylation directs p300/CBP-mediated histone acetylation at DNA double-strand breaks to facilitate repair. *Nat. Commun.* **10**, 4951–14 (2019).
42. F. Gong *et al.*, Screen identifies bromodomain protein ZMYND8 in chromatin recognition of transcription-associated DNA damage that promotes homologous recombination. *Genes Dev.* **29**, 197–211 (2015).